

# Dynamical thickening transition in plate coating with concentrated surfactant solutions

Jérôme Delacotte<sup>1</sup>, Lorraine Montel<sup>1</sup>, Frédéric Restagno<sup>1</sup>, Benoît Scheid<sup>2</sup>, Benjamin Dollet<sup>3</sup>, Howard A. Stone<sup>4</sup>, Dominique Langevin<sup>1</sup>, and Emmanuelle Rio<sup>1</sup>

<sup>1</sup> Laboratoire de Physique des Solides UMR8502, Université Paris-Sud - 91405 Orsay, France, EU

<sup>2</sup> TIPs - Fluid Physics unit, Université Libre de Bruxelles - C.P. 165/67, 1050 Brussels, Belgium, EU

<sup>3</sup> Institut de Physique de Rennes UMR6251, Université de Rennes - 35042 Rennes, France, EU

<sup>4</sup> Department of Mechanical and Aerospace Engineering, Princeton University, Princeton, NJ 08544, USA

## Abstract

We present a large range of experimental data concerning the influence of surfactants on the well-known Landau-Levich-Derjaguin experiment where a liquid film is generated by pulling a solid plate out of a bath. The thickness  $h$  of the film was measured as a function of the pulling velocity  $V$  for different kind of surfactant and at various concentrations. Measuring the thickening factor  $\alpha=h/h_{\text{LLD}}$ , where  $h_{\text{LLD}}$  is obtained for a pure liquid, in a wide range of capillary ( $Ca=\eta V/\gamma$ ), two regimes of constant thickening can be identified: at small capillary number,  $\alpha$  is large due to a confinement and surface elasticity (or Marangoni) effects and at large  $Ca$ ,  $\alpha$  is slightly higher than unity, due to surface viscous effects. At intermediate  $Ca$ ,  $\alpha$  decreases as  $Ca$  increases along a “dynamic transition”. In the case of non-ionic surfactants, the dynamic transition occurs at a fixed  $Ca$ , independently of the surfactant concentration, while for ionic surfactants, the dynamic transition depends on the concentration due to the existence of an electrostatic barrier. The control of physico-chemical parameters allowed us to elucidate the nature of the dynamic transition and to relate it to surface rheology.

# 1. Introduction

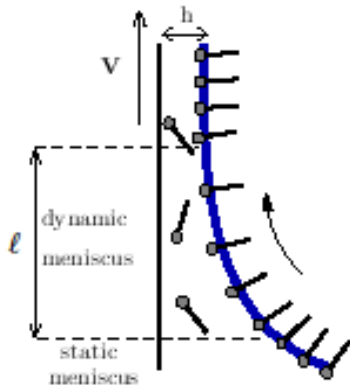
When a solid object is pulled out of a liquid reservoir, a thin layer of liquid is entrained by viscous drag. Since coating flows are ubiquitous in industrial processing, understanding the variables that control the film thickness is of major importance. In industrial processes, the coatings can be made of pure liquid such as oils, but can also be paints, emulsions, polymers solutions, i.e. complex fluids. The coating materials protect, functionalize, and lubricate surfaces. In most cases, it is desirable to obtain a well controlled thickness of the applied layer and a high coating speed to maintain a high throughput. Therefore it is of interest to determine the dependence of thickness of these thin films on physico-chemical parameters. In this paper we report experimental results of solid plates coating by various types of surfactant solutions in a wide range of concentrations above the cmc. Our results are compared to available theoretical models.

The classic film-coating theory by Landau-Levich and Derjaguin (LLD) uses the lubrication and low capillary number approximations and then solves the governing equations by matching the thin film region (of constant thickness  $h$ ) far away from the bath with the static meniscus (near the horizontal bath) through an intermediate transition region called the "dynamical meniscus" of length  $\ell$  (Levich 1962), as illustrated in Figure 1. The calculation is based on an asymptotic matching approach, and a numerical calculation is used to obtain the film thickness:

$$h_{LLD} = 0.9458 \ell_c Ca^{2/3}, \quad (1)$$

where  $Ca = \eta V/\gamma$  is the capillary number,  $V$  the plate velocity, and  $\eta$  and  $\gamma$  respectively the viscosity, and the surface tension of the liquid into air;  $\ell_c = \sqrt{\gamma/\rho g}$  is the capillary length, with  $\rho$  the density of the liquid. Physically, equation (1) means that increasing the velocity of the plate or the viscosity of the liquid leads to an increase of the drag force, and then to a thicker film. On the other hand, increasing the surface tension of the liquid decreases the film thickness. This calculation imposes a no-slip boundary condition at the solid-liquid interface and zero tangential stress at the liquid-air interface. The LLD calculation is valid for  $Ca^{1/3} \ll 1$  since when the capillary number is close to one, gravitational effects cannot be neglected (Derjaguin 1943) (note that this condition becomes  $Ca^{1/3}Bo \ll 1$  in cylindrical geometries). We will work in the small  $Ca$

61 regime in the present paper. For a liquid of viscosity  $\eta = 10^{-3}$  Pa.s, a surface tension  $\gamma$  between 30  
 62 and 40 mN/m, and a density  $\rho = 10^3$  kg/m<sup>3</sup>, the film thickness is predicted to vary from 17 nm to  
 63 20  $\mu$ m, if  $V$  varies from 1  $\mu$ m/s to 40 mm/s ( $2.5 \times 10^{-8} < Ca < 10^{-3}$ ).



64  
 65  
 66 **Figure 1: Velocity controlled withdrawal of a solid plate out of a liquid bath. The air-liquid interface is**  
 67 **stretched in the so-called dynamic meniscus, which has an extension  $\ell$  and connects the static meniscus with**  
 68 **the flat film region. In the dynamic meniscus, the viscous drag is balanced by surface tension forces. In the**  
 69 **case of a surfactant solution, Marangoni effects and interfacial viscous effects can also be important.**  
 70

71 There are only a few experimental validations of the LLD law for simple liquids. In a  
 72 planar configuration. Krechetnikov and Homsy (2005, 2006) measured the thickness of the liquid  
 73 films by measuring the weight of the entrained liquid. Using glycerol-water solutions over a wide  
 74 range of  $Ca$ ,  $10^{-3} < Ca < 10^{-1}$ , they reported agreement with equation (1), with small corrections  
 75 for a finite bath size and an overall accuracy of 10 %. In particular, the power law of  $\frac{2}{3}$  was  
 76 verified with an accuracy of 5%. Note that in the case of pure liquids with a substrate of  
 77 controlled roughness, they observed a significant thickening of the films relative to those on  
 78 smooth substrates and a different power of capillary number than predicted in equation (1). More  
 79 recently, Snoeijer et al. (2008) reported a precise validation of the LLD law for silicon oil and a  
 80 wetting surface. The thickness of the film was measured using an interferometric technique, and  
 81 the precision was as good as 0.2 %. We note that the authors also showed that in the case of  
 82 partial wetting, another solution different than the LLD law exists, which has a larger film  
 83 thickness and scales as  $\ell_c Ca^{1/2}$ .

84 Most coating flow experiments involving withdrawal of a substrate have been performed  
 85 on curved surfaces such as the coating of fibers ( ) or capillary tubes (Chen 1986, Schwartz et al.  
 86 1986). The thickness of the withdrawn film is then given by the Bretherton law, which is a

87 variant of the LLD law (Bretherton 1961). Indeed, since the radius of curvature in the static  
88 meniscus is directly given by the tube radius  $r$  rather than by  $\ell_c/\sqrt{2}$  (if  $r \ll \ell_c$ ), the Bretherton  
89 law is  $h = 1.34 r Ca^{2/3}$ . The film thickness in fiber coating obeys the same law, taking  $r$  for the  
90 fiber radius.

91 .

92 Several studies have indicated deviations from the LLD law when complex fluids are  
93 used. We will only recall here the experiments made with solutions containing surface-active  
94 substances. In the plate drag-out problem, Groenveld used water-glycerol solutions containing  
95 traces of hexane or oil and measured films thicker than predicted by the LLD law (Groenveld  
96 1970). Recently, Krechetnikov and Homsy (2005) reported experiments using sodium dodecyl  
97 sulfate (SDS) solutions whose critical micellar concentration (cmc, concentration above which  
98 micelles form) is 8.3 mM. They observed that the film tends to thicken when a surfactant is  
99 added (the ratio  $c/cm_c$  was varied between 0.2 and 1). They defined, as other authors in other  
100 geometries, a thickening factor  $\alpha$  which is the ratio of the measured film thickness  $h$  to the film  
101 thickness predicted by the LLD relation:

$$102 \quad \alpha = \frac{h}{h_{LLD}} . \quad (2)$$

103 The theoretical thickness  $h_{LLD}$  was calculated by using in equation (1) the surface tension of the  
104 surfactant solution  $\gamma$  measured at equilibrium at the specified bulk concentration. For a  
105 Newtonian fluid,  $\alpha=1$ ; Krechetnikov and Homsy (2005) found  $\alpha = 1.55$ , independently of  $Ca$  in  
106 the range  $10^{-4}$ - $10^{-3}$  and of the surfactant concentration. Note finally that Krechetnikov and Homsy  
107 (2006) numerically predicted thinning of the withdrawn film, in qualitative disagreement with the  
108 experiments. However, systematic values of the sorption rates would be required to check  
109 whether such a thinning is general. Moreover, Campana et al. (2010) proposed a numerical  
110 simulation that predicts a thickening due to surfactant and could rationalize the experimental  
111 results of Krechetnikov and Homsy (2005). It remains therefore unclear what is the role of the  
112 sorption barriers in the general case.

113 The largest amount of experimental data concerns fiber coating. To our knowledge all the  
114 experiments have shown a thickening due to surfactants. For this geometry, the thickening factor

115  $\alpha$  has been shown to depend on the chemical nature of the surfactant, on the surfactant  
116 concentration, on the radius of the fiber, and on the capillary number. The most extensive study  
117 has been done with SDS solutions (Quere 1998, 1999): the thickening factor ( $\alpha$ ) was measured as  
118 a function of concentration, it was observed to increase before the cmc and reach a maximal  
119 value of 2.2 around the cmc, and eventually to decrease to a constant value of 1.6 between 1 and  
120 10 cmc. In the same paper, a single set of experiments is reported with a different surfactant,  
121 dodecyl trimethyl ammonium bromide (DTAB). A dynamic thickening transition is then  
122 observed by increasing the capillary number (increasing the withdrawal velocity), after which the  
123 thickening factor  $\alpha$  decreased toward unity. In this article, we choose to investigate this dynamical  
124 transition of thickening. We then did systematic experiments with concentrated surfactants both  
125 ionic and non ionic, which is of large importance, as it will be stated in the following.

126  
127 Note that many other experiments exhibiting data far away from the LLD (or Bretherton)  
128 power-law are available in the literature, most of them dealing with the bubble-in-a-tube or fiber  
129 geometry. Many different mechanisms can be invoked for such a deviation: gravity effects appear at  
130 high capillary numbers (White 1965), the circular shape intrinsic to the bubble experiment can also  
131 lead to deviations at small capillary numbers (Schwartz 1986). Last but not least, such a transition  
132 has also been observed in the bubble-in-a-tube geometry, using pure liquids (Bretherton 1961, Chen  
133 1986), where it is suggested that a very small amount of surfactants, leading to strong gradients, is  
134 at the origin of this transition. None of these mechanisms can be invoked to explain our experiments  
135 since we are working with concentrated surfactants, at small capillary numbers and in a flat  
136 geometry.

137  
138 The thickening is usually ascribed to the Marangoni effect, i.e. a surface concentration  
139 gradient leading to an additional stress at the surface. This Marangoni effect can be made  
140 quantitative by introducing the surface elasticity. The surface compression elastic modulus,  $E$ , is  
141 defined as:

142 
$$E = -A \frac{d\Pi}{dA} ,$$

143 where  $A$  is the surface area,  $\Pi = \gamma_w - \gamma$  the surface pressure, with  $\gamma_w$  the surface tension of pure

144 water.  $E$  is interpreted as the 2D analog of a 3D compression bulk modulus  $-\partial p/\partial \mathcal{V}$ , where  $p$  is  
145 the pressure and  $\mathcal{V}$  the volume. For insoluble surfactants,  $E = \Gamma \frac{d\Pi}{d\Gamma}$ , with  $\Gamma$  the surface  
146 concentration of surfactant. The surface compression process can be accompanied by friction in  
147 the surface layer, in which case, a two-dimensional compression surface viscosity  $\eta_E$  is  
148 introduced. Note that shear can also be applied, in which case, a shear modulus  $S$  and a shear  
149 viscosity  $\eta_S$  need to be introduced.

150 When soluble surfactants are used, the problem is more complicated since exchanges between  
151 surface and bulk are possible. When the time scale of the compression is comparable to the  
152 exchange time between the bulk and surface, the resistance to compression is lowered and the  
153 apparent elastic modulus  $E$  is smaller than the value only due to the monolayer at the interface.  
154 There is a significant dissipation associated with the surface-bulk exchange, and the apparent  
155 surface viscosity  $\eta_S$  is much larger than the value intrinsic to the monolayer (Stevenson 2005).  
156 Elasticity as well as viscosity then depends not only on the surfactant concentration but also on  
157 the perturbation time scale of the interface. The values of  $E$  and  $\eta_S$  tend to decrease significantly  
158 at high concentration and/or at low frequency since surfactants have time to exchange between  
159 surface and bulk. This variation has been modeled by Levich (1962) and by Lucassen and van  
160 den Tempel (1972). Note also that soluble surfactant monolayers usually flow under shear  
161 stresses, for which we expect that the shear elastic modulus  $S$  is zero and the shear viscosity  $\eta_S$  is  
162 small. Stebe et al. studied the remobilization of surfaces in a three-phase slug flow (Stebe  
163 1991). They showed that at high surfactant concentration or at a high transport rate of  
164 surfactants, a uniform concentration of surfactant at the interfaces leads to a response similar  
165 to a clean interface (with a lower surface tension). There has been an important theoretical  
166 effort to model the effect of an interfacial stress at the interface and its consequence in a  
167 coating experiment. Most of this effort has been concentrated on the Bretherton geometry.  
168 Park (Park 1991) and Chang and Ratulowski (1990) studied the deviation from Bretherton's  
169 results in the case of small amounts of surfactants. Stebe and Barthès-Biesel (1995) studied the  
170 case of elevated surfactant concentrations. All of these theoretical works conclude that when  
171 the surface elasticity and/or viscosity increase there exists an upper bound on the film  
172 thickness, which is  $4^{2/3}$  times the value obtained by Bretherton with pure liquids.

173  
174  
175 In the case of coating processes, another feature to be considered is the film thickness: if  
176 the film is too thin, it cannot act as a reservoir of surfactant for the surface (Lucassen 1981).  
177 Quéré and de Ryck introduced the dimensionless number  $\sigma = \Gamma/(ch)$ , which compares the amount  
178 of surfactant at the surface with the amount of surfactant in the film, where  $\Gamma$  is the surface  
179 concentration and  $c$  is the bulk concentration. If  $\sigma \gg 1$ , there is not enough surfactant in the film  
180 to replenish the surface during film stretching; in this case, the elastic modulus  $E$  is much larger  
181 than that of the surface of a solution with the same surfactant concentration, and is rather close to  
182 the intrinsic elastic modulus  $E_0$  (Lucassen 1981). Note that Quéré and de Ryck attributed the  
183 observed dynamical transition of thickening to the transition between regimes with  $\sigma \gg 1$  and  
184  $\sigma \ll 1$ . However, in their experiments the transition occurred around  $\sigma = 10^{-2}$  and not unity. We  
185 will discuss this apparent contradiction below.

186 It is always difficult to separate the role of surface viscosities and elasticities. The film  
187 response is never purely elastic as assumed in the models based on Marangoni effects. It is never  
188 purely viscous either. In a previous paper (Scheid 2010), we chose particular experimental  
189 conditions to be only sensitive to the intrinsic surface viscosity effects. We showed that at high  
190 concentrations of surfactant and at capillary numbers above the dynamical transition of  
191 thickening, a thickening effect of about 6% was observed with DeTAB, which could thus be  
192 rationalized by the sole effect of the intrinsic surface viscosity.

193 Despite the present knowledge on coating problems, many important questions regarding  
194 coating with surfactant solutions still remain to be understood. For example, little is known about  
195 the film thickness variation with surfactant concentration well above the critical micellar  
196 concentration and about the role of surfactant solubility and the surface rheology on the film  
197 thickness. In this article, we focused on this situation (role of surface rheology at large surfactant  
198 concentration) and describe a set of systematic experiments with several surfactant solutions. We  
199 study the film thickening properties of a non-ionic surfactant, C<sub>12</sub>E<sub>6</sub>, and two cationic surfactants,  
200 DeTAB and DTAB. A comparison between the experimental results and the existing theories is  
201 made.

202

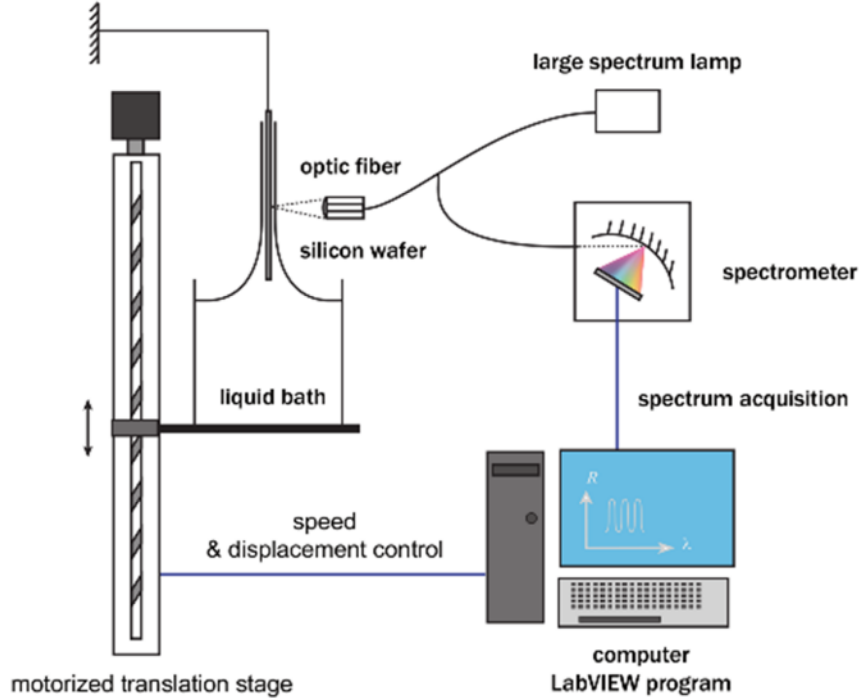
203  
204  
205  
206  
207  
208  
209  
210  
211  
212  
213  
214  
215  
216  
217  
218  
219  
220  
221

## 2. Experiments

### 2.1 Apparatus and methods

We built an experimental set-up that allows controlling the film formation and measuring its thickness. A translation stage (Newport UTS 150CC) coupled with a controller (Newport SMC100CC) was used to drive a bath of solution down with a controlled velocity ( $1 \mu\text{m/s}$ - $40 \text{ mm/s} \pm 1\mu\text{m/s}$ ). The film thickness was measured using an interferometric technique. A white light beam is reflected by both interfaces of the film and analyzed using a spectrometer. Both the light source (LS-100) and the spectrometer (USB 400) are Ocean Optics devices. The range of wave lengths span from 450 to 900 nm. The apparatus is shown in Figure 2. Silicon wafers (Siltronix 111) were used as solid plates for the withdrawal experiments. They exhibit low roughness at the atomic scale and were cleaned, just before each experiment, using both piranha solution and UV-ozone cleaner to ensure good wettability. To avoid any edge effects, the measurements are made in the middle of the wafer which has a size around 5 cm in each direction. The thickness is measured above the dynamic meniscus, at a distance around two times the capillary length from the horizontal surface in order to be in the flat zone of the entrained film.





222  
 223 **Figure 2: Experimental set-up for film coating.** A translation stage moves the bath of solution with a controlled  
 224 velocity. The plate is coated by a liquid film whose thickness is measured using a spectrometer. The  
 225 reflectivity is recorded as a function of the wavelength of light.  
 226

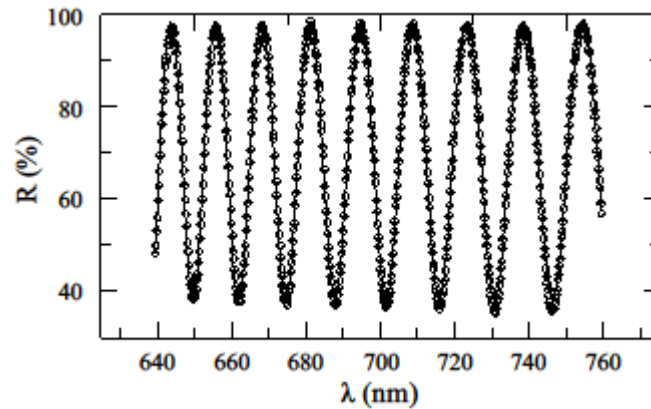
227 The raw data, i.e. the reflectivity  $R$  as a function of the wavelength, was monitored with  
 228 the Spectrasuite interface software from Ocean Optics. The film thickness was determined, with  
 229 5% accuracy, by adjustment of the data using the following expression (Born and Wolf 1985):

$$230 \quad R = b \frac{\left(\frac{n^2 - 1}{2n}\right)^2 \sin^2\left(2\pi \frac{nh}{\lambda}\right)}{1 + \left(\frac{n^2 - 1}{2n}\right)^2 \sin^2\left(2\pi \frac{nh}{\lambda}\right)} + d, \quad (3)$$

231 where  $h$ ,  $\lambda$  and  $n$  are, respectively, the film thickness, the wavelength and the refractive index of  
 232 the solution. The latter was measured with a refractometer (OPL) after each experiment. No  
 233 correction is required for the presence of the surfactant monolayers (whose thickness is of the  
 234 order of 1nm) since  $h$  is of the order of microns. Fitted parameters are  $b$ ,  $d$  and  $h$ . Note that  $b$  and  
 235  $d$  could have been expressed as functions of the refractive indices of the silicon wafer and the  
 236 solution. We used them as fitting parameters to make the procedure simpler. In order to make the  
 237 adjustment less sensitive to the initial value of  $h$ , some researchers use a simple cosine function  
 238 (Snoeijs 2008). Figure 3 shows an example of the thickness determination for a surfactant

239 solution.

240



241

242 **Figure 3 : Reflectivity spectrum recorded from the spectrometer with the Spectrasuite software (dots) and fit**  
243 **with equation (3) (line) for a film made of a 990 mM DeTAB solution. The film thickness obtained in this**  
244 **example is  $h=12.7 \mu\text{m}$ , and other parameters are  $b=640.1$ ,  $d=38.1$ , with  $n=1.374$ .**

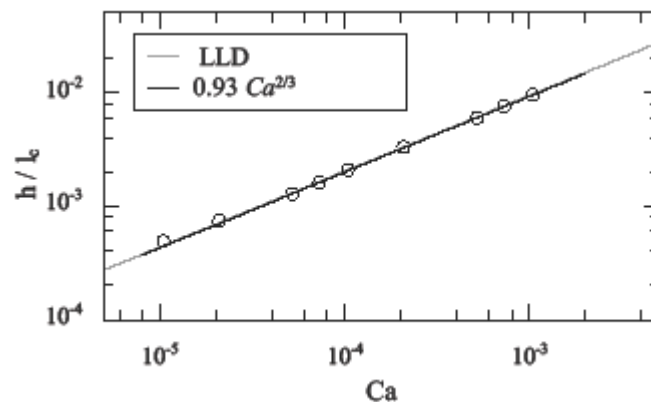
245

246 The validation of the experimental set-up was made with a pure liquid, whose properties are easy to  
247 control. We chose a silicon oil (Rhodorsil 47V20) instead of water, since the surface of water is difficult  
248 to keep uncontaminated after several withdrawals of a plate, even with careful handling and filtration.

249 Figure 4 shows the film thickness scaled by the capillary length  $\ell_c$  as a function of the capillary number  
250  $Ca = \eta V / \gamma$ ; we use logarithmic scales, throughout this paper.

251 In this figure, the dashed line corresponds to the mean value for the thickening factor,  $\alpha =$   
252  $0.99$ , which is 1% below the theoretical value, lying in turn within the standard deviation of 2%. The  
253 error on the thickness measurement was then evaluated at a maximum value of 5% (including  
254 reproducibility), which is beyond the size of the experimental points in all of the figures.

255



256

257 **Figure 4 : Validation of the experimental set-up by using a silicon oil 47V20 ( $\eta = 20$  mPa.s,  $\gamma = 21$  mN/m). The**  
258 **film thickness  $h$  is well predicted by the LLD model, equation (1).**  
259

## 260 **2.2 Materials**

261  
262 We used three different surfactants in order to vary the distribution of surfactant  
263 molecules between the bulk and the surface of the film: dodecyl trimethyl ammonium bromide (  
264 DTAB), decyl trimethyl ammonium bromide (*De*TAB) and hexaethyleneglycol-  
265 monododecylether ( $C_{12}E_6$ ). Their critical micellar concentrations (cmc) are given in table 1.  
266 DTAB was purchased from Sigma-Aldrich and was recrystallized three times before use in order  
267 to decrease the amount of impurities. *De*TAB (purity 99 %) and  $C_{12}E_6$  (purity 98 %) were  
268 purchased from Sigma-Aldrich and used as delivered. Note that DTAB is very stable against  
269 hydrolysis, and, to avoid chemical decomposition and solution aging, we always used freshly  
270 prepared solutions of  $C_{12}E_6$ , which hydrolyses only very slowly (on the time scale of a week). Water  
271 used in the experiments was ultra-purified water from a Millipore-Q instrument (resistivity = 18  
272 M $\Omega$  cm).

273

surfactant	cmc (mM)	$\gamma_{\text{cmc}}$ (mN/m)	$\ell_c$ (mm)
$C_{12}E_6$	0.07	32.3	1.82
DTAB	15	38.0	1.97
<i>De</i> TAB	66	39.7	2.01

274

275 **Table 1: Critical micellar concentration (cmc) of the three surfactants used in this study, together with the**  
276 **surface tension measured at the cmc (with an experimental error of  $\pm 0.5$  mN/m), and the capillary length**  
277 **calculated with the density of the solution at the cmc.**

278

279 Surfactant  $C_{12}E_6$  has the lowest monomer solubility (corresponding to the lowest cmc) since it  
280 is nonionic (Durbut 1999). The viscosities of all surfactant solutions were measured with a low  
281 shear rheometer (Low Shear 30 Contraves) at a temperature of 25°C at which the experiments have  
282 been conducted. Viscosities of  $C_{12}E_6$  solutions were comparable to that of water for the all range  
283 of surfactant concentration. Measured viscosities for ionic surfactants (DTAB and *De*TAB)

284 reached somewhat larger values (up to 3.35 mPa.s) when the concentration was increased, which  
285 are still low enough to exclude the presence of wormlike micelles or liquid crystalline phases in  
286 the bulk (Israelachvili 1992). The surface tensions were measured for all solutions using a  
287 Wilhelmy plate apparatus, with an accuracy of 0.5 mN/m.

288  
289 As mentioned in the introduction, we are working at very small capillary numbers for which  
290 gravity is negligible, i.e.  $Ca^{1/3} \ll 1$ . Moreover, with a maximum velocity of 40 mm/s, the Weber  
291 number that compares inertial to capillary effects is  $We = \rho V^2 l_c / \gamma \approx 10^{-1} \ll 1$ . Hence inertial  
292 effects are also negligible here.”

293

294

## 295 **3. Results and discussion**

296

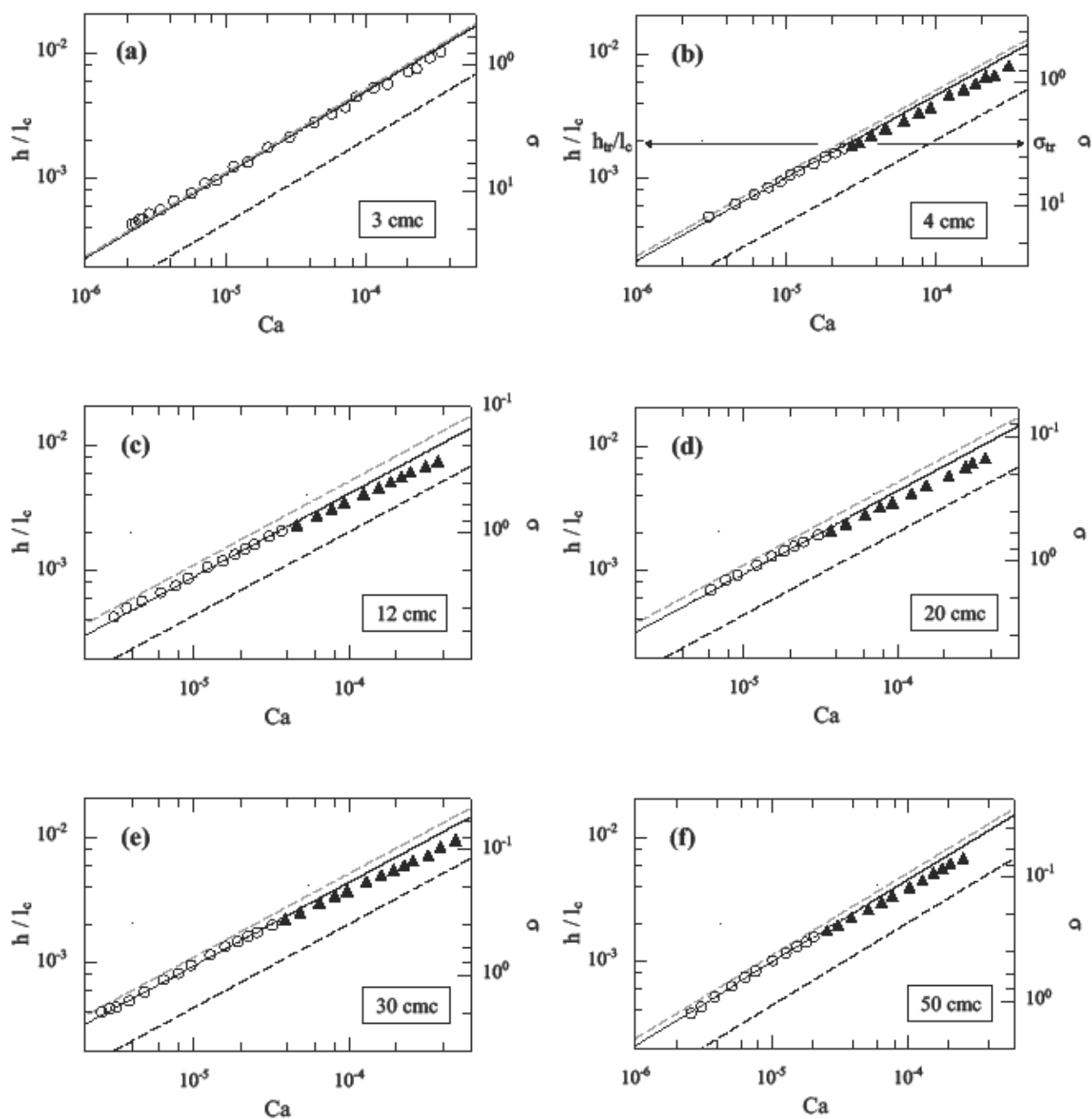
297 In this section, we present the results obtained by varying the type of surfactant and the  
298 concentration. The film thickness was measured as a function of the capillary number and  
299 concentration.

300

### 301 **3.1 Non-ionic surfactant**

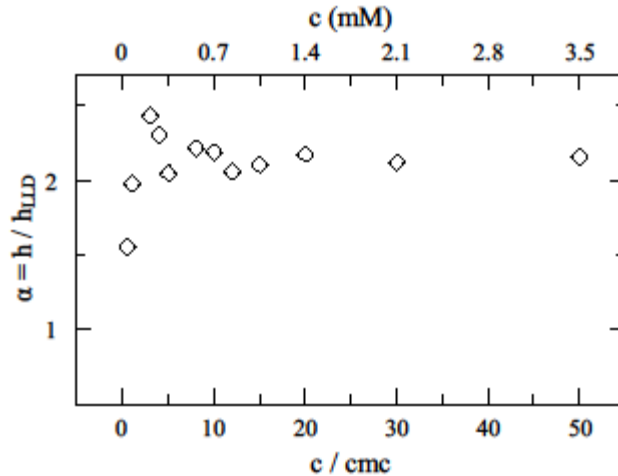
302

303 The concentrations of C<sub>12</sub>E<sub>6</sub> solutions spanned from 0.07 to 3.5 mM (i.e., in the range 1 –  
304 50 cmc). Figure 5 shows the variation of film thickness ( $h$ ) rescaled by the capillary length ( $l_c$ ) as  
305 a function of the withdrawal velocity ( $V$ ) expressed in terms of the dimensionless capillary  
306 number ( $Ca$ ). At small concentration (0.21 mM, or 3cmc, as shown in Figure 5(a)), a constant  
307 thickening factor  $\alpha$  is observed in the range of investigated  $Ca$ . Indeed, the film thickness varies  
308 as the 2/3 power of the velocity. At these concentrations (Figure 5(a)),  $\alpha$  is close to  $\alpha_{\max} = 4^{2/3}$ . At  
309 higher concentrations (0.28 mM or 4 cmc and above, see Figure 5(b) - Figure 5(f)), we still  
310 observe a constant  $\alpha$  for low thicknesses (i.e. low capillary numbers). However, when the film  
311 thickness increases, a transition occurs:  $h \propto Ca^{2/3}$  is no longer observed and the thickening factor  
312 decreases. In this transition regime, the thickness variation as a function of the velocity agrees  
313 well with another power law  $h \propto Ca^{1/2}$ , as noted by Ou Ramdane and Quéré (1998). Whatever the  
314 concentration, the transition occurs around the same capillary number  $Ca \approx 3 \times 10^{-5}$ , which is  
315 associated with a film thickness  $h \approx 3.8 \mu\text{m}$ .



317 **Figure 5: Film thickness rescaled by the capillary length plotted as a function of the capillary number for**  
 318 **various concentrations. The results correspond to various  $C_{12}E_6$  concentrations in the solution (with a cmc of**  
 319 **0.07 mM). The right vertical axis shows the value of  $\sigma$  (increasing from top to bottom) corresponding to each**  
 320 **thickness. The dashed lines, bold and normal, show respectively the LLD thickness ( $\alpha=1$ ) and the maximum**  
 321 **possible thickness ( $\alpha=4^{2/3}$ ) corresponding to an immobile interface. Solid line is a fit over the constant**  
 322 **thickening region from which the value of  $\alpha$  is obtained. Open and filled symbols represent data in the**  
 323 **constant thickening region and in the thickening transition region, respectively. The subscript “tr” denotes**  
 324 **parameters taken at the intersection between these two regions as represented in (b).**  
 325

326 The values of constant thickening  $\alpha$  found at low capillary number are shown in figure 6 for each  
 327 concentration:  $\alpha$  first increases with concentration and then saturates above 0.21 mM (3 cmc) to  
 328 a value  $\alpha \approx 2.1$ .



329  
 330 **Figure 6 : Thickening factor  $\alpha$  versus  $C_{12E_6}$  concentration rescaled by the cmc (0.07 mM).**

331  
 332 In order to reach higher concentrations without having elongated micelles or liquid crystalline  
 333 phases (and larger viscosities that could vary with the velocity  $V$ , thus complicating the  
 334 interpretation), we studied short chain cationic surfactants, for which we next report the results.

335

## 336 **3.2 Ionic surfactants**

337

### 338 **3.2.1 DTAB**

339

340 The DTAB concentration was varied in a range spanning from 10 to 375 mM (i.e. 2/3 to  
 341 25 cmc). The experimental trends are qualitatively similar to those with  $C_{12E_6}$ . As shown in  
 342 Figure 7(a) - Figure 7(d), for concentrations up to 150 mM (10 cmc),  $\alpha$  remains constant when  
 343  $Ca$  is varied. At higher concentrations a transition in film thickening is observed: the thickening  
 344 factor decreases toward values close to the LLD prediction (see Figure 7(e) - (f)). The transition  
 345 occurs above  $Ca \approx 10^{-4}$  and  $h \approx 6 \mu\text{m}$ . These values are similar to those obtained with  $C_{12E_6}$   
 346 ( $3 \times 10^{-5}$  and  $4 \mu\text{m}$ , respectively).

347

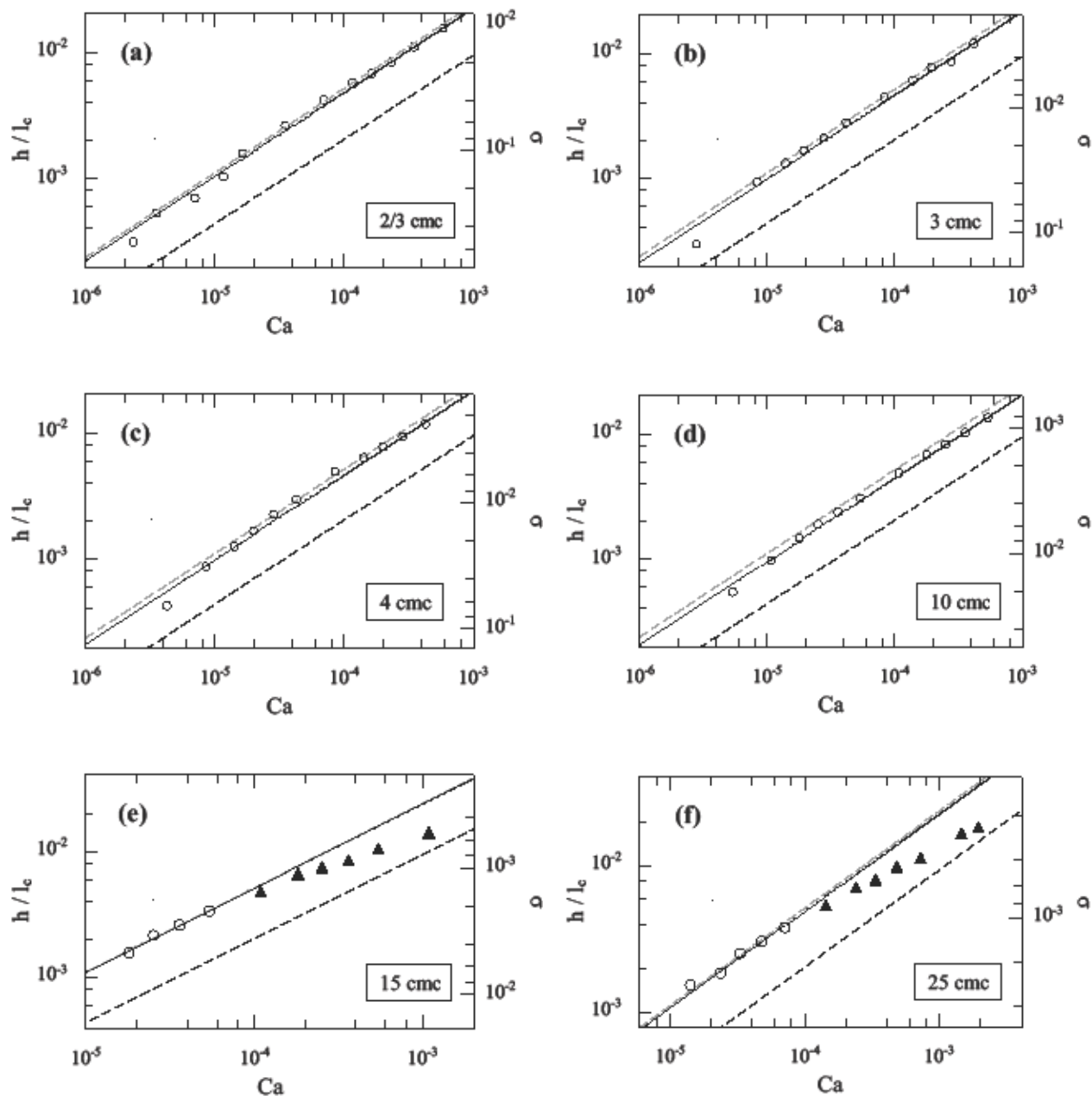
348

349

350

351

352



353

354

355

Figure 7: Results obtained with DTAB for various concentrations (with a cmc of 15 mM). Same axes and notations as for Figure 5.

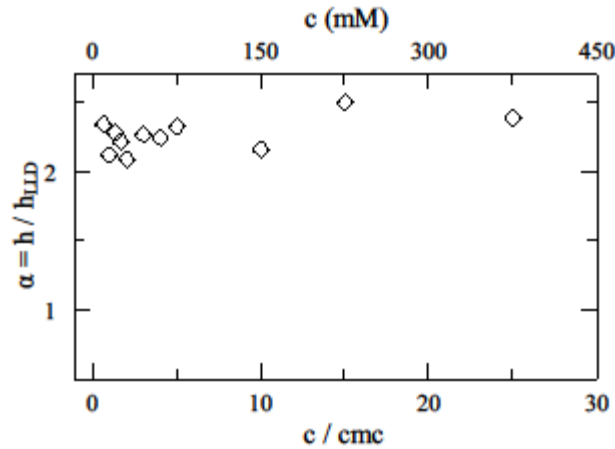
356

357

358

In Figure 8, we plot the thickening factor variation with surfactant concentration at low  $Ca$ . As for  $C_{12}E_6$ , the thickening factor, for higher concentrations is the constant value obtained before the thickening transition (i.e. for small capillary numbers). Here  $\alpha$  remains high and nearly

359 constant when the concentration is varied.

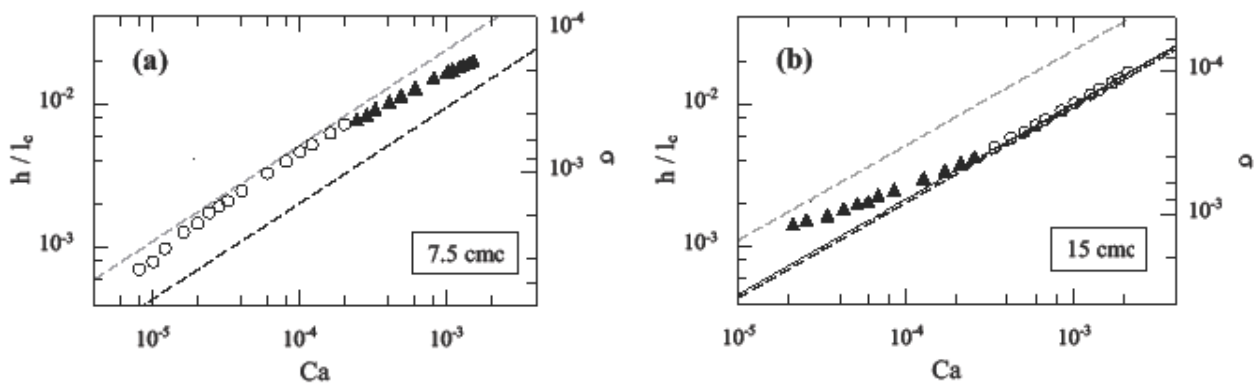


360  
361 Figure 8: Thickening factor  $\alpha$  for DTAB versus concentration rescaled by the cmc (15 mM).  
362

### 363 3.2.2 DeTAB

364  
365 In order to investigate large surfactant concentrations, we chose to use DeTAB which  
366 allows the viscosity to remain small and constant in the entire range of investigated  $Ca$  values. As  
367 shown in Figure 9(a), the beginning of the thickening transition is observed with a 495 mM (i.e.,  
368 7.5 cmc) solution. With twice this concentration, 990 mM (i.e., 15 cmc) (Figure 9(b)) the end of  
369 the thickening transition is visible. The thickening factor is constant at high  $Ca$  values and  
370 slightly greater than unity (the LLD prediction):  $\alpha = 1.06 \pm 0.05$  (Scheid et al. 2010).

371



372 Figure 9: Results obtained for DeTAB for two concentrations (with a cmc of 66 mM). Same axes and notations  
373 as for Figure 5.  
374

375  
376



377

### 378 **3.3 Interpretation**

379

380 In the following section, we will discuss the observed dynamical transition. As stated in the  
381 introduction, a similar transition was already observed in another study in the fiber geometry <sup>4</sup> but  
382 no systematic measurements in which surfactants and surfactant concentration are varied in a large  
383 range have been performed.

384 As explained in the introduction, the thickening factor depends on the surface  
385 viscoelasticity, hence on the flow characteristics through the capillary number. More  
386 specifically, “the dynamic transition of thickening” is linked to the replenishment of the surface  
387 by surfactants. Many mechanisms are in competition here: transport of surfactants by diffusion  
388 and/or convection towards the interface as well as their adsorption/desorption. Moreover, the  
389 film thickness and the surfactants concentration are also very important since a small thickness  
390 and/or small concentration can prevent the surfactant remobilization through the confinement  
391 effect (see section ...)

392 First of all, let us discuss diffusion and adsorption. One reason why we consistently observe  
393 a large thickening may be that surfactants do not have enough time to reach the surface during the  
394 experiment. Nevertheless, convection is always efficient enough to replenish the surface (Quére  
395 1998, Shen 2002): incompressibility of the liquid allows the mass conservation equation  $\nabla \cdot \mathbf{u} = 0$ ,  
396 to be approximated as  $V/\ell \sim v_t/h$ , where  $V$ ,  $\ell$ ,  $v_t$  and  $h$  are, respectively, the withdrawal velocity, the  
397 dynamic meniscus extension, the characteristic transverse velocity in the film and the film  
398 thickness. As a result,  $h/v_t$  which is the time required to convect surfactants across the entire film  
399 is comparable to the time  $l/V$  required for the surfactant to go through the entire dynamic  
400 meniscus. Diffusion can also play a role for very thin films. The time necessary to diffuse  
401 through the film is  $h^2/D$  where  $D \sim 5 \cdot 10^{-10}$  m<sup>2</sup>/s is the diffusion coefficient of the surfactants. The  
402 convection and diffusion times are of the same order of magnitude when  $V \approx \ell D/h^2$  (note that this  
403 is equivalent to the calculation of a Péclet number comparing diffusion and convection times),  
404 which corresponds to  $Ca = ((\eta D)/(\gamma \alpha^3 \ell_c))^{1/2} \approx 3 \times 10^{-5}$  (using  $\ell \approx \ell_c \alpha^{1/2} Ca^{1/3}$  and  $h \approx \alpha \ell_c Ca^{2/3}$ ). So  
405 at small capillary numbers, diffusion may play a role while it becomes negligible at large  $Ca$ . In  
406 any case, any surfactant present into the film has enough time to reach the surface during the

407 experiment by either convection or by diffusion. So, the other mechanisms are limiting in our case.  
408 The thickness and concentration effects are then discussed in paragraphs 3.3.1 and 3.3.2 whereas  
409 the adsorption is discussed in paragraph 3.3.2.

410

### 411 **3.3.1 Film thickness effects**

412

413 Let us first focus on apparent surface viscoelasticity variations with film thickness. This  
414 point was quantitatively addressed by Lucassen and coworkers (Lucassen 1972, 1981, Lucassen-  
415 Reynders 1969). Their model is based on an analogy between a surface perturbed during a very  
416 short time, where the surfactant motion is limited by diffusion and a thin film in which surface  
417 replenishment is instantaneous. When the surface of a semi infinite solution is perturbed during a  
418 short time, surfactants can be exchanged between bulk and surface due to diffusion. The diffusion  
419 coefficient of surfactant molecules is assumed to be constant from the bulk up to the surface and  
420 the solution dilute enough so that no micelles are present. If the surface of the solution is  
421 stretched quickly, diffusion is not fast enough to replenish the interface and the surface  
422 viscoelastic moduli are increased. On the contrary, if the expansion is very slow, surfactant  
423 concentration gradients are rapidly smoothed out by diffusion of surfactant from the bulk toward  
424 the interface, and the surface viscoelastic moduli are decreased.

425 The refilling efficiency can be quantified by the length scale  $(D\tau_e)^{1/2}$  over which surfactants can  
426 be remobilized due to diffusion during the expansion time  $\tau_e$ , where  $D$  is the diffusion coefficient  
427 of the surfactant. This length scale can be used to relate the thin film surface viscoelastic moduli  
428 as a function of thickness to the surface viscoelastic moduli of the bulk solution as a function of  
429 expansion time: the surface elasticity of a thin film is the same as that of a solution for an  
430 expansion time  $\tau_e$ , if the film thickness  $h$  is equal to  $(D\tau_e)^{1/2}$ . The surface elastic moduli are small  
431 at low frequency (large  $\tau_e$ ) and large at high frequency (small  $\tau_e$ ), with the transition frequency  
432 increasing with concentration<sup>11</sup>. Consequently, the film elastic modulus decreases when  $h$   
433 increases, as expected from the surface-film analogy (Prins 1967). We then expect a high  $\alpha$  at  
434 small film thicknesses which is actually observed (Figure 5). Unfortunately, it is impossible to  
435 extract a quantitative expression for the thin film elasticity since our experiments are performed  
436 at very high concentration at which micelles are present. The relation between  $c$  and  $\Gamma$  is not  
437 known precisely, so we are unable to calculate the surface elastic moduli variations of a solution

438 with respect to time of expansion and concentration and predict the characteristic thickness at  
439 which this transition is supposed to occur. However, we carried out systematic measurements of  
440 the thickening factor ( $\alpha$ ), obtained before the dynamical transition of thickening (if any), with  
441 respect to C<sub>12</sub>E<sub>6</sub> and DTAB concentration ( $c$ ) (Figure 6 and Figure 8, respectively). In both cases,  
442 we observe very reproducible large thickening factors ( $\alpha > 2$ ) for concentration at and above the  
443 cmc which shows that the confinement (or thickness) effect is very robust.

444

### 445 3.3.2 Transition from large to small thickening

446

447 The occurrence of a thickening transition, when increasing solution concentration or film  
448 thickness, is a general behavior that was observed with all three surfactants. It had also been  
449 observed on withdrawn fibers in the presence of DTAB by Quéré and co-workers (1998). As  
450 these authors suggested, the solution must be concentrated enough to allow the refilling of the  
451 interface during film formation in the dynamic meniscus. The dynamic meniscus acts as a  
452 surfactant reservoir with a thickness that increases with  $Ca$ . Therefore, for a given concentration,  
453 at low film thickness (i.e., low  $Ca$ ), a shortage of surfactants can be expected, resulting in an  
454 increase of apparent surface viscoelastic moduli. In turn, beyond a threshold thickness, the  
455 reservoir contains enough surfactant to refill the interface, which results in a decrease of the  
456 apparent surface viscoelastic moduli. This “confinement effect” is the basis of the calculation of  
457 the film elastic modulus of Prins and coworkers discussed in section 3.3.1. The transition  
458 observed is then a confinement effect.

459 As stated in the introduction, Quéré and de Ryck (1998) introduced a dimensionless  
460 number  $\sigma$  to estimate the capacity of the bulk to act as a surfactant reservoir. This parameter  
461 compares the amount of surfactant molecules adsorbed at the interface and present in the  
462 dynamic meniscus, and is given by  $\sigma = \Gamma / (ch)$ . In Figure 5, Figure 7 and Figure 9, the right vertical  
463 axes give  $\sigma$  calculated with  $\Gamma \approx 2$  molecules/nm<sup>2</sup>, which is a typical value for the surfactants used  
464 at  $c \geq \text{cmc}$  (Israelachvili 1992). As can be seen in Figure 5, in the case of C<sub>12</sub>E<sub>6</sub> the thickening  
465 transition occurs when  $\sigma$  is of order unity, which is when the amount of surfactant molecules in  
466 the dynamic meniscus is of the same order of magnitude as the amount of adsorbed molecules. In  
467 the case of DTAB (see Figure 7), the thickening transition occurs, more surprisingly, around  $10^{-3}$ ,  
468 suggesting that here the “confinement effect” (for small film thickness) is not the only effect

469 involved as discussed in the next section.

470

### 471 **3.3.3 Adsorption barrier effects**

472

473 In the case of ionic surfactants, the thickening transition occurs at higher  $Ca$  and  $h$  values  
474 and for higher bulk concentrations ( $\sigma \ll 1$ ). Let us note that the dynamic transition of thickening  
475 observed by Ou Ramdane and Quéré (1998) for DTAB also occurred well below  $\sigma = 1$ . This  
476 response could be due to adsorption electrostatic barriers associated with the charged surfactant  
477 monolayers present at the surface. Such a barrier indeed leads to an increase of the time necessary  
478 for the surfactants to reach the surface by an exponential factor  $\exp(W/k_B T)$ , where  $W$  is the  
479 adsorption energy barrier,  $k_B$ , the Boltzmann constant and  $T$  the absolute temperature. For DTAB  
480 close to the cmc,  $W \sim 15 k_B T$  (Ritacco 2011). Addition of salt lowers the energy barrier  
481 (electrostatic screening), which disappears above salt concentrations of about 100mM. Addition  
482 of large amounts of ionic surfactant produces a similar self screening effect, which is expected to  
483 lead to the disappearance of the barrier as well. The effective compression elastic modulus of  
484 dilute ionic surfactant solutions is much larger than predicted by the Lucassen-van den Tempel  
485 model at high surfactant concentrations, but decreases and tends towards the values predicted by  
486 the model when enough salt is added (Bonfillon 1994). This observation could account for the  
487 fact that the thickening transition is observed for much larger surfactant bulk concentrations in  
488 the case of ionic surfactants than with nonionic surfactants.

489 We then propose that, below 100mM, even though the surfactants are available at high enough  
490 concentration and have time to reach the surface, the electrostatic barrier prevents them from  
491 adsorbing. So, as soon as  $W$  is large enough to prevent adsorption, it is reasonable to assume that  
492 the surfactants cannot adsorb at the interface, leading to large effective elasticity and then a large  
493 thickening factor. Now, this effect of electrostatic barrier decreases with increasing surfactant  
494 concentration (like for the salt in the example above).

495

### 496 **3.3.4 Concentration effects**

497

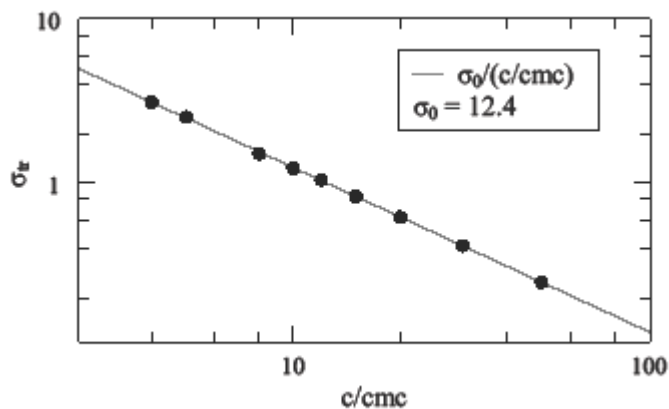
498 In this last section, we look at the concentration effects on the dynamical transition of  
499 thickening, focusing on the experimental results with  $C_{12}E_6$  for which no adsorption barrier

500 effects are expected. Provided the thickening transition is due to the confinement effects gauged  
 501 by the parameter  $\sigma$  (see section 3.3.1 and 3.3.2), we report in Figure 10 the value of this  
 502 parameter at the beginning of the transition, denoted  $\sigma_{tr}=\Gamma/(ch_{tr})$ , versus the scaled concentration  
 503  $c/cmc$ , with  $h_{tr}$  the thickness at the transition (see Figure 5 (b)). The logarithmic fit of the data  
 504 represented by the solid line in Figure 10 gives

$$505 \quad \sigma_{tr} = \frac{\sigma_0}{c/cmc}, \quad (4)$$

506  
 507 where  $\sigma_0 \approx 12.4$  is the fitting constant. Assuming  $\sigma_0$  to be independent of the concentration down  
 508 to the cmc, we can write  $\sigma_0=\Gamma/(cmc \cdot h_{tr})$ . Taking a typical value of  $\Gamma = 1$  molecule/ $50\text{\AA}^2$  (i.e.,  
 509  $\Gamma \approx 3 \times 10^{-6}$  mol/m<sup>2</sup>), with  $cmc = 0.07$  mM, we find  $h_{tr} \approx 3.5$   $\mu$ m, which matches the observations  
 510 in Figure.5. Now, using the surface-film analogy, we can extract a typical frequency equivalent to  
 511 this value of the film thickness at the transition:  $f_{tr}=D/h_{tr}^2 \approx 40$  Hz, where  $D = 5 \times 10^{-10}$  m<sup>2</sup>/s.

512  
 513



514  
 515 **Figure 10: Values of the parameter at the beginning of the transition  $\sigma = \sigma_{tr}$  (see Figure 5 (b)) as a function of**  
 516 **concentration of  $C_{12}E_6$  scaled by cmc, and fit (solid line) with equation (4).**

517  
 518 Our experiments then show that, at a frequency higher than 40Hz (i.e. at a thickness smaller than  
 519 3.5  $\mu$ m), the surface elasticity saturates at a high value. Some experiments have been done by  
 520 Stubenrauch et al. (2009) to measure directly the surface elasticity of  $C_{12}E_6$  around the cmc at  
 521 small frequencies (below 1Hz). The authors extrapolate their results at high frequency and  
 522 observe a saturation of the surface elasticity around few tens of Hertz. We think that what we  
 523 observe in our experiment corresponds to this saturation of surface elasticity at high frequency.

524 Unfortunately, to our knowledge, no measurements at concentrations higher than the cmc and at  
525 high frequency are available in literature. These measurements, using capillary waves to reach  
526 high frequencies, are beyond the scope of this paper.

527  
528 The transition from large to small thickening is determined by the bulk concentration of  
529 surfactant.. In this “classical” transport picture, the micelle disassembly provides a “source” of  
530 monomer and the transport of the surfactants into or out of the micelle is not taken into account.  
531 Due to their small size, surfactants diffuse to the surface much faster than the micelle and, in the  
532 case of low micelle concentration a depletion zone can appear. The concentration of surfactant at  
533 the interface then depends on micelle break-down kinetics. Maldarelli and coworkers (Bhole  
534 2010, Song 2002) have studied this effect both experimentally and theoretically. At large  
535 surfactant concentrations (as in our experiment), this effect can be neglected as micelle  
536 breakdown is extremely fast.

537  
538

## 539 **4. Conclusion**

540 This work provides an extensive experimental study of solid coating in the plate geometry while  
541 varying the type of surfactant and concentration. Our experiments show two main features:

- 542 • First, we confirmed repeatedly the thickening of the withdrawn liquid film with respect to the  
543 LLD prediction for every concentration and in the entire range of  $Ca$  for which gravity is  
544 negligible.
- 545 • Second, we provided evidence of two regimes separated by a dynamical thickening  
546 transition. At small capillary number, the film thickness is very small and a confinement  
547 effect can be observed. Then, at a thickness predicted by the dimensionless number  $\sigma$  for  
548 nonionic surfactants, the confinement effect disappears and  $\alpha$  slowly evolves towards the  
549 LLD prediction. At very high concentration and thickness, this transition ends and a small  
550 remaining thickening is observed, due to intrinsic surface viscosity, as explained in our  
551 previous paper (<sup>13</sup>).

552 The thickening effects and transitions are driven by interfacial rheological properties

553 coupled to surface refilling mechanisms. Moreover, thickening transitions seem to be a general  
554 feature in thin films made of surfactant solutions. Elasticity of the interface is the main source of  
555 thickening in the case of interfacial surfactant concentration gradients, as it is the case for either  
556 low concentrations or films with low thickness, whereas, for intermediate concentrations or  
557 thicker films, interfacial viscosity also plays a role.

558 For non ionic surfactants, the thickening transition occurs for  $\sigma$  of order unity. This  
559 feature is not true anymore for the ionic surfactants and we suggest that this behavior is due to an  
560 electrostatic barrier that prevents the adsorption of surfactants at small concentration and thus  
561 shifts the thickening transition towards higher bulk concentrations.

562  
563 **Acknowledgements** We are grateful to Isabelle Cantat and Ernst van Nierop for  
564 numerous helpful discussions. We also thank François Boulogne for valuable help with  
565 experimental set-up. BS acknowledges the Brussels region for financial support through the  
566 program “Brains Back to Brussels” as well as the FRS-FNRS.

567  
568 .  
569

## 570 **References**

- 571 BONFILLON A. AND LANGEVIN D., Electrostatic model for the viscoelasticity of ionic surfactant  
572 monolayers, *Langmuir*, **10**, 2965 (1994).  
573  
574 BORN AND WOLF, Principles of Optics 6<sup>th</sup> Ed., *Pergamon Press*, **7** (1985).  
575  
576 BRETHERTON F.P., The motion of long bubbles in tubes, *J. Fluid Mech.*, **10**, 166 (1961).  
577  
578 CAMPANA D. M. ET AL., Numerical prediction of the film thickening due to surfactants in the  
579 Landau-Levich problem, *Phys. Fluids*, **22**, 032103 (2010).  
580  
581 CHEN J.-D., Measuring the film thickness surrounding a bubble inside a capillary, *J. Colloid*  
582 *Interface Sci.*, **109**, 341 (1986).  
583  
584 DERJAGUIN B., On the thickness of the liquid film adhering to the walls of a vessel after emptying,  
585 *Acta physico-chim. USSR*, **20**, 349 (1943).  
586  
587 DURBUT P., Handbook of detergents, Part A: Properties, surfactant science series, ch3, *Marcel*  
588 *Dekker*, **82** (1999).

589  
590 GEORGIEVA D. ET AL., Link between surface elasticity and foam stability, *Soft Matter*, **5**, 2063  
591 (2009).  
592  
593 GROENVELD P., Low capillary number withdrawal, *Chem. Eng. Sci.*, **25**, 1259 (1970).  
594  
595 ISRAELACHVILI J., Intermolecular and Surface Forces 2<sup>nd</sup> Ed., *Academic Press* (1992).  
596  
597 KRECHETNIKOV R. AND HOMSY G. M., Experimental study of substrate roughness and surfactant  
598 effects on the Landau-Levich law, *Phys. Fluids*, **17**, 102108 (2005).  
599  
600 KRECHETNIKOV R. AND HOMSY G. M., Surfactant effects in the Landau-Levich problem, *J. Fluid*  
601 *Mech.*, **559**, 429 (2006).  
602  
603 LANDAU L. AND LEVICH B., Dragging of a liquid by a moving plate, *Acta Physicochim. USSR*, **17**,  
604 42 (1942).  
605  
606 LANGEVIN D., Influence of interfacial rheology on foam and emulsion properties, *Adv. Colloid*  
607 *Interface Sci.*, **88**, 209 (2000).  
608  
609 LEVICH V. G., Physicochemical Hydrodynamics., *Prentice-Hall*, (1962).  
610  
611 LUCASSEN, J., Anionic surfactants: physical chemistry of surfactant action. Surfactant science  
612 series., chapter Dynamic Properties of Free Liquid Films and Foams, *Marcel Dekker*, **11**, 217  
613 (1981).  
614  
615 LUCASSEN J. AND VAN DEN TEMPEL M., Dynamic measurements of dilational properties of a  
616 liquid interface, *Chem. Eng. Sci.*, **27**, 1283 (1972).  
617  
618 LUCASSEN-REYNDERS E. H. AND LUCASSEN J., Properties of capillary waves, *Adv. Colloid*  
619 *Interface Sci.*, **2**, 347 (1969).  
620  
621 OU RAMDANE O. AND QUÉRÉ D., Thinning factor in Marangoni coating, *Langmuir* **13**, 2911  
622 (1997).  
623  
624 PARK C.-W. Effects of insoluble surfactants on dip coating, *J. Colloid Interface Sci.* **146**, 382  
625 (1991).  
626  
627 PRINS A. ET AL., Elasticity of thin liquid films *J. Colloid Interface Sci.* **24**, 84 (1991).  
628  
629 QUERE D. AND DE RYCK A., Le mouillage dynamique des fibres, *Ann. Phys. (Paris)*, **23**, 1 (1998),  
630 QUÉRÉ D., Fluid coating on a fiber, *Ann. Rev. Fluid Mech.*, **31**, 347 (1999).  
631  
632 RATULOWSKI J. AND CHANG H. C., Marangoni effects of trace impurities on the motion of long  
633 gas bubbles in capillaries, *J. Fluid. Mech.*, **210**, 303 (1990).  
634  
635 RITACCO H. ET AL., Dynamic surface tension of aqueous solutions of ionic surfactants: role of



636 electrostatics, *Langmuir*, in press.  
637  
638 SCHEID B. ET AL., The role of surface rheology in liquid film formation, *Europhys. Lett.* **90**,  
639 24002 (2010).  
640  
641 SCHWARTZ L. W., PRINCEN, H. M.; KISS, A. D., On the motion of bubbles in capillary tubes, *J.*  
642 *Fluid Mech.*, **172**, 259 (1986).  
643  
644 SHEN A. ET AL., Fiber coating with surfactant solutions, *Phys. Fluids*, **14**, 4055 (2002).  
645  
646 SNOEIJER J. H. ET AL., Thick films of viscous fluid coating a plate withdrawn from a liquid  
647 reservoir, *Phys. Rev. Lett.*, **100**, 244502 (2008).  
648  
649 STEBE K. J. ET AL., Remobilizing surfactant retarded fluid particle interfaces. I. Stress-free  
650 conditions at the interfaces of micellar solutions of surfactants with fast sorption kinetics., *Phys*  
651 *Fluids A.*, **3**, 3 (1991).  
652  
653 STEBE K. J. ET AL., Marangoni effects of adsorption-desorption controlled surfactants on the  
654 leading end of an infinitely long bubble in a capillary, *J. Fluid Mech.*, **286**, 25-48 (1995).  
655  
656 STEVENSON P., Remarks on the shear viscosity of surfaces stabilised with soluble surfactants, *J*  
657 *Coll. Int. Sc.*, **290**, 603-606 (2005)  
658  
659 STUBENRAUCH C. ET BARTHES-BIESEL D., Aqueous foams stabilized by *n*-dodecyl- $\beta$ -D-  
660 maltoside, hexaethyleneglycol monodecyl ether, and their 1:1 mixture., *Soft Matter*, **5**, 3070  
661 (2009).  
662  
663 TCHOLAKOVA S. ET AL., Comparison of solid particles, globular proteins and surfactants as  
664 emulsifiers, *Phys. Chem. Chem. Phys.*, **10**, 1608 (2008).  
665  
666 WHITE, D. A.; TALLMADGE, J. A., Theory of drag out of liquids on flat plates. *Chemical*  
667 *Engineering Science* **1965**, 20 (1), 33-37.  
668  
669